Differential peat deformation, compressibility, and water storage between peatland microforms: Implications for ecosystem function and development

J. M. Waddington,[1] E. Kellner,[1,2] M. Strack,[3] and J. S. Price[4]

Received 21 October 2009; revised 2 March 2010; accepted 12 March 2010; published 29 July 2010.

[1] Because peat is elastic, the daily to seasonal swelling and shrinking of the peat surface not only affects water storage but also alters peatland hydraulics and the biogeochemical and thermal properties of peat. Due to different botanical origins and degrees of decomposition, we hypothesized that different peatland microforms (ridges and lawns) display a large variation in peat deformation and compressibility. Here we examined the spatial variation of peat surface movement, peat strength, and volumetric water content at a low lawn (LL), upper lawn (UL), and ridge (R) along a 5 m transect in a peatland in Quebec, Canada. The average seasonal amplitude in peat surface level was 9, 6, and 2 cm at the LL, UL, and R sites, respectively. The surface layers in each of these sites were fairly rigid with the largest changes in peat thickness occurring between 20 and 60 cm depth in the peat profile. Compressibility varied among microforms but was not correlated to other properties within the layer in individual soil layers. However, when average profile compressibility was considered, it was significantly correlated to peat depth, von Post humification, distance to hollow, and peat strength. The total water storage by dilation below the water table was about the same as the water deficit (precipitation minus evapotranspiration) for LL, while the storage deficit for UL and especially R was lower. Including changes in entrapped gas content over the season reduced estimates of changes in water storage at all sites. Because microform type and position were significant predictors of hydrophysical properties, we argue that this suggests that peatland microtopography is self-reinforcing through ecohydrological feedbacks. Including the variability in these properties in peatland ecohydrological models will be key for predicting the response of peatland ecosystems to disturbance.

Citation: Waddington, J. M., E. Kellner, M. Strack, and J. S. Price (2010), Differential peat deformation, compressibility, and water storage between peatland microforms: Implications for ecosystem function and development, *Water Resour. Res.*, *46*, W07538, doi:10.1029/2009WR008802.

1. Introduction

[2] The net long-term sink of atmospheric carbon dioxide (CO_2) in peatlands [*Gorham*, 1991; *Turunen et al.*, 2002] is controlled to a large extent by the water table position [*Gorham*, 1995] and the long mean residence time of water in these ecosystems. Lateral water flow in peatlands are limited due to their low hydraulic gradients, the steep decline (3–5 orders of magnitude) in hydraulic conductivity (K_{sat}) with depth [*Whittington and Price*, 2006], and the common occurrence of microtopographic features (microforms) [*Price and Maloney*, 1994]. The physical characteristics of these microforms (e.g., hummocks, hollows, ridges, and lawns) create an ecohydrological feedback where water flows and stores are a consequence of the hydraulic and mechanical properties [*Whittington and Price*, 2006] that arise from their position and alignment in the landscape [*Foster et al.*, 1983; *Price and Maloney*, 1994]. This in turn controls the vegetation community [*Rydin and Jeglum*, 2006], which then controls the development of a peatland through complex interactions between peat quality, hydrological conditions [*Belyea and Baird*, 2006], and decomposition rates [*Belyea and Clymo*, 2001] in the peat from which the microforms are composed. Consequently, characterizing the relationship between microform type and peat hydraulic and mechanical properties is essential to understanding flows and stores of water, nutrients, and carbon [e.g., *Waddington and Roulet*, 2000]. However, quantifying the relevant fluxes and stores of water is confounded by the short-term and long-term temporal variability of the governing variables. It has long been recognized that peat properties change over the long term as decomposition proceeds [*Belyea and Baird*, 2006]. More recently, it has been demonstrated that there is a strong seasonal variability of peat hydraulic conductivity resulting from deformation of the matrix as water pressure varies, subsiding as water storage is reduced, and dilating when it is gained [*Price*,

[1]School of Geography and Earth Sciences, McMaster University, Hamilton, Ontario, Canada.
[2]Midvatten AB, Borlange, Sweden.
[3]Department of Geography, University of Calgary, Calgary, Alberta, Canada.
[4]Department of Geography and Environmental Management, University of Waterloo, Waterloo, Ontario, Canada.

0043-1397/10/2009WR008802

2003; *Whittington and Price*, 2006]. The susceptibility of different microforms to deformation was noted by *Whittington and Price* [2006], who found peat volume change diminished in the order lawns > hollows > ridge. However, they did not establish quantifiable relationships between peat type, strength, and compressibility, which is the aim of this study. Here we quantify the spatial and temporal variability of peat deformation, peat strength, compressibility, and water storage in different peatland microforms along a hollow ridge transect during a growing season in a Québec peatland. On the basis of previous studies that suggest that a significant part of the water budget is accounted for by dilation storage [*Price and Schlotzhauer*, 1999; *Koerselman*, 1989; *Pyatt and John*, 1989], as the peat column swells to accommodate increased water storage and compresses with pore drainage, we hypothesized that hummocks/ridges, owing to higher degree of decomposition and shrubby vegetation composition, would have greater peat strength and demonstrate lower peat deformation and compressibility and changes in water storage relative to adjacent lawns. Furthermore, because entrapped gas can decrease the effective stress caused by the weight of the overlying material on a soil layer [*Strack et al.*, 2006], we also hypothesize that entrapped gas could affect the pattern of peatland microform peat deformation and water storage. For example, *Kellner et al.* [2005] demonstrated that entrapped gas overpressuring may develop where gas production is high, replacing water in pore spaces with bubbles, thereby reducing water storage. While we would expect that hollows and lawns would have a higher methane production than ridges due to greater carbon quality [*Strack et al.*, 2005], recent evidence suggests that ridges may trap more CH_4 [*Strack and Mierau*, 2010], likely due to greater peat strength. We also hypothesized that peat microform compressibility would be related to differences in physical parameters such as bulk density, root density, fiber content, and the degree of decomposition. While *Price et al.* [2005] found no relationship between peat compressibility and these peat properties, their measured compressibility in the laboratory was different than field measurements of compressibility. We hypothesized that the field compressibility is a consequence of both the peat properties in the vertical profile and in the adjacent areas that help to strengthen the overall peat mass.

[3] The specific objectives of this study were to quantify the spatial and temporal variability of peat deformation, peat strength, compressibility, and water storage in different peatland microforms along a hollow ridge transect during a growing season in a Québec peatland. Understanding the factors that contribute to differences in microform compressibility and water storage is necessary so that these controls can be built into the next generation of process-based peatland (eco)hydrological models, where cross-scale feedbacks are important to peatland development and ecosystem function [*Belyea and Baird*, 2006].

2. Materials and Methods

2.1. Study Area

[4] This study was carried out in a poor, open fen site (46°40′N 71°10′W) close to the village of St. Charles de Bellechasse, Québec, Canada (46°75′N, 70°98′W). The study area is a relatively undisturbed 3 ha remnant of a patterned fen peatland whose surrounding area has been drained and vacuum harvested for horticultural peat over the previous 10 years. Near the middle of the peatland remnant, we instrumented a 5 m transect from a hollow, populated by *Sphagnum majus* with a sparse cover of *Rhynchospora alba* and *Carex* spp. to a ridge with *Sphagnum rubellum*, *Andromeda polifolia*, and *Chamaedaphne calyculata* shrubs. Between the hollow and ridge, there was an approximately 2 m wide *Sphagnum papillosum* and *Sphagnum magellanicum* lawn showing a slight topographic gradient from the wetter conditions in the hollow end to the drier end where the lawn intersects with the ridge. Along the transect, we established three measurement sites: a "low lawn" site (or LL) situated approximately 0.5 m from the hollow, an "upper lawn" site (UL), which was located about 1 m from LL, and 1 m farther along the transect was a ridge site (R). LL and UL had the same moss species cover, although the UL vascular plant vegetation included more *Andromeda polifolia* and less *Rhynchospora alba* than LL. Mean peat depths at the LL, UL, and R sites were 1.13, 1.22, and 1.60 m, respectively. The total elevation difference along the entire length of the transect was ~0.3 m, and the mean peat surface level at the LL, UL, and R sites at the start of the study period were 1.46, 1.50, and 1.60 m (above an arbitrary datum), respectively.

[5] Measurements of peat surface position, water table position, and pore water pressure were made at six subsites at each of the LL, UL, and R sites (i.e., 18 sites total) from day of year (DOY) 141 to 245, which represented most of the 2003 growing season. At the end of the study period, we also measured peat strength and collected peat samples for peat property analysis in the laboratory.

2.2. Precipitation and Evapotranspiration

[6] Air temperature, precipitation (tipping bucket), net radiation, and ground heat flux were measured every 20 min with a Campbell Scientific CR10X data logger at a meteorological station approximately 50 m from the study site. Daily evapotranspiration was estimated with the *Priestley and Taylor* [1972] combination model calibrated with soil lysimeters located at LL, UL, and R sites. Details are provided by *Whittington and Price* [2006].

2.3. Peat Surface and Water Table Position

[7] Water table was measured continuously at LL and R with a counterbalanced pulley on a potentiometer connected to a Campbell Scientific CR10X data logger that measured each minute and averaged every 20 min; and manual measurements were made at the UL and R sites. Unfortunately, early in the field season, the R potentiometer failed, so only manually measured water levels could be used for analysis. Peat surface levels were provided from manual measurements of the vertical distance between a fixed sight wire, and the peat surface at each of the 18 subsites. Peat levels were measured at each of the 18 subsites using manual elevation sensor rods [*Price*, 2003] inserted at depths of 20, 40, and 60 cm and one automated continuously recording set of elevation sensor rods at depths 0, 20, 30, 50, and 70 cm at each of the LL and UL sites, whereas only the surface level was monitored automatically at the R site. The automated sensor rods were attached with nylon monofilament line to potentiometers that were connected to the data logger. Manual measurements of peat level were made 2 times per week by viewing the position of elevation rods that extended above the soil surface against a stable datum (a sight wire fixed to anchor

rods that were sunk into the underlying clay substrate). The change in peat volume in each layer (strain) was determined from the change in elevation between sequential elevation sensor rods. Strain (e) can thus be expressed as

$$e = \frac{\Delta z}{\Delta z_o}, \quad (1)$$

where Δz is the thickness of a layer at depth z and Δz_o is the thickness of the layer at the beginning of measurements.

2.4. Volumetric Water Content

[8] Volumetric water content (θ) was measured in one of the subsites at each site using Campbell Scientific CS615 moisture probes (Campbell Scientific, Inc., Logan, UT). The probe length was 30 cm, and the probes were installed horizontally at 25 cm depth and vertically at 25–55 and 45–75 cm depths in all three subsite profiles. This type of sensor uses time domain measurement methods that are sensitive to dielectric permittivity (ε), although the way to determine ε is slightly different from traditional TDR (time domain reflectometry) technique [*Bilskie*, 1997]. The dielectric permittivity was calculated from the instrument signal τ, a probe specific offset $\tau_{\rm offset}$, and the measured signal value in air τ_a,

$$\varepsilon = ((\tau - \tau_{\rm offset})/(\tau_a - \tau_{\rm offset}))^2. \quad (2)$$

Using a mixing model expression [*Birchak et al.*, 1974], θ for each probe was expressed as

$$\theta = \frac{\varepsilon^\alpha - (1-\eta)\varepsilon_m^\alpha - \eta\varepsilon_a^\alpha}{\varepsilon_w(T)^\alpha - \varepsilon_a^\alpha}, \quad (3)$$

where ε with subscripts m, a, and w denote the dielectric permittivity for the peat, air, and water, respectively, T is temperature, η is porosity of the soil [L^3 L^{-3}], and α is a parameter expressing the geometry of the soil, determined to 0.35 [*Kellner and Lundin*, 2001]. Although careful calibration of each sensor was carried out in the laboratory, the uncertainty in absolute values was ±5%. However, the uncertainty in changes of θ at each probe was ±1%.

2.5. Water Storage

[9] The water storage S in the saturated zone to a depth of 75 cm for each profile was calculated as

$$S = \sum_{z=-75}^{-20} \theta z \Delta z. \quad (4)$$

Only the measured water contents between 20 and 75 cm depths were considered. Both the deeper layers and the unsaturated zone are excluded from the calculation. The lowest seasonal water table level was at ~20, 25, and 30 cm depths at LL, UL, and R profiles, respectively. With this in mind, the moisture probes were assumed to be consistently below the water table or within the capillary fringe and therefore should represent saturated conditions. Thus, any changes in water content in these layers should be due to changes in dilation storage or free phase gas volume.

[10] The change in volumetric gas content γ was calculated as

$$\Delta\lambda = (\eta - \eta_0) - (\theta - \theta_0), \quad (5)$$

where θ is measured water content and η is porosity, estimated as

$$\eta = 1 - \frac{(1-\eta_0)L_0}{L}, \quad (6)$$

where L is layer thickness and subscripts 0 denote the initial values for the season.

[11] While entrapped gas has been shown to be localized in nature [e.g., *Kellner et al.*, 2005], gas contents in the saturated zones of the measured subsite profiles were assumed to be representative for all subsite profiles at each site as gas content may influence the peat volume.

2.6. Pore Water Pressure

[12] Pore water pressure was automatically recorded using nonvented pressure transducers (KPSI 173, Pressure Systems, Inc., Hampton, VA) buried in the peat at depths of 25, 40, and 60 cm in the same profiles as the moisture probes. The insertion cavities were sealed with peat mud for the first 10 cm and then with a 10 cm bentonite plug to deter preferential flows of gas and water.

[13] Pore water pressure was also measured using tensiometers (installed to 30 and 50 cm depths) consisting of plastic tubes supplied with a porous plate in the bottom end and sealed with a rubber septum at the upper end. Manual measurements were taken twice a week using a pressure transducer (accuracy of ±1 mb) (Soil Measurement Systems, Tucson, AZ). Measured pressure values were converted to actual pressure and total head (cm) based on the height of the water column in each tensiometer and its depth below the peat surface.

2.7. Peat Compressibility

[14] Peat compressibility or the coefficient of volume change (m_v) was determined as the slope of the relationship between the change in vertical strain (∂e) and effective stress ($\partial\sigma'$):

$$m_v = \partial e/\partial\sigma'. \quad (7)$$

Strain was calculated using equation (1).

[15] Using a one-dimensional approach, the effective stress in a layer at depth $z = \Sigma\Delta z_u + \Sigma\Delta z_s$, where Δz_u and Δz_s are the thicknesses of the unsaturated and saturated zones above the layer, can be expressed as

$$\sigma'_z = \sum_{u=1}^{m} [(\rho_p(1-\eta_u) + \rho_w\theta_u)]g\Delta z_u + \sum_{s=1}^{n} [(\rho_p - \rho_w)(1-\eta_s) + (\rho_g - \rho_w)\gamma_s]g\Delta z_s, \quad (8)$$

where ρ_p, ρ_w, and ρ_g are the densities of peat, water, and gas, respectively; g is acceleration due to free fall; η is porosity; θ is water content; γ is gas volume; and subscripts m and n refer to the number of layers in the unsaturated and saturated zones, respectively.

[16] Peat compressibility was calculated for the layers between the monitored levels at 10, 20, 40, and 60 cm depth as well as for the peat column below 60 cm depth. The depth-integrated compressibility, expressed as the season-

averaged slope of the relationship between the change in surface level and water table level, was also determined for each monitored profile.

2.8. Peat Strength

[17] At the end of the study period, we measured peat strength at each of the 18 subsites using a penetrometer. The penetrometer was made of a 1.5 m long, 10 mm diameter iron rod and covered with electrical tape to make it slide easier in the peat. This tape added to the rod ensured that any increase in friction as the penetrometer was lowered into the peat was minimal. The bottom end of the penetrometer was finished with a round shape while the top end of the penetrometer was flat. The penetrometer was "hit" by dropping a 1.5 kg sledgehammer head onto the top end from a fixed 5 cm height. The number of hits required to drop the penetrometer a depth of 5 cm into the peat was recorded for every 5 cm interval from the peat surface to mineral soil at all 18 subsite peat profiles.

2.9. Peat Properties

[18] Peat cores (~30 cm long, 20 cm wide, and 80 cm deep) were removed from each of the 18 subsites at the end of the field season. Cores were placed in aluminum frames during sampling to facilitate stability, sealed in plastic bags to retain moisture, frozen, and then transported to the Ecohydrology Research Laboratory at McMaster University for further analysis.

[19] We determined root and fiber content at 15, 25, 35, and 45 cm depths for each of the 18 peat profiles. All intact fibers were categorized into groups of high rigidity (material with high lignin content) or low rigidity (mosses and flexible roots). Fibers were classed as highly rigid if they offered inflexible resistance to bending before snapping. Second, the fibers were categorized into diameter groups of <1, 1–3, and >3 mm using a ruler for measurement. Finally, the length of the fibers was recorded. These three procedures facilitated an approximation of both the fibric content volume of the peat samples relative to the total sample volume and the rigidity of the samples.

[20] The peat sample used for root density and fiber analysis was then used to determine the bulk density ρ_d. The whole sample was dried at 75°C and then weighed. We estimated the degree of decomposition using the von Post humification scale as presented by *Clymo* [1983] using the average of two to three subsamples of peat of undefined volume.

2.10. Statistical Analyses

[21] In order to investigate the role of microform type and depth as descriptors of peat properties such as compressibility, bulk density, and peat strength, analysis of variance (ANOVA) was conducted using the General Linear Model in Minitab according to a repeated measures design (Minitab Statistical Software, Version 14). Depth, microform type, and depth × microform interaction were included as potential sources of variability. All data were checked for normality, and nonnormally distributed data were transformed using the box-cox power transformation prior to analysis. Differences in peat properties averaged over the depth of the profile were also assessed between microforms using a one-way ANOVA with Tukey's pairwise comparisons. We also assessed correlations between these depth-integrated average properties using Pearson correlation analysis. In all statistical tests, an α value of 0.05 was used to indicate significance. Our overall research design was pseudoreplicated [*Hurlbert*, 1984], because it was not feasible to replicate the instrumentation at other sites and precaution was taken in the interpretation of the data.

3. Results

3.1. Water Table Position and Volumetric Water Content

[22] The water table level range was 33 cm over the study period and generally reflected the variations in weather during the season (Figure 1). A relationship between manually measured levels at LL and R ($WT_R = 1.1446 \times WT_{LL} - 18.6$, all in centimeters; $r^2 = 0.99$) indicated that the water table at R (WT_R) was 7–11 cm below the LL water table (WT_{LL}), with a smaller difference when the water table was high. Consequently, it is worth noting that there was a general slope in water table from LL toward R, because this was the slope of the peatland.

[23] In the first few weeks of the measurement period, the weather was fairly wet. After DOY 165, there was a drier period during the midsummer until about DOY 202, when it started to get wetter again. At DOY 216, there was a significant rain event yielding 70 mm rain during which the water table rose over 25 cm. While the patterns of θ were generally related to the variation in water table levels (Figure 2), several exceptions to this occurred. For example, θ decreased 5%–10% (generally continuously) during the growing season at the R profile, with a greater response at depth. The decrease in θ was quicker in the drier period between DOY 165 and 200 (Figure 2) and did not recover significantly during the following relatively wet period (e.g., after rainstorm of DOY 216). At the UL profile, θ decreased at all three levels, generally corresponding to the water table variation. LL profile θ varied in a similar pattern to that at UL but the variations were greater. The greatest change in θ occurred at 25 cm depth in the LL profile, where the total change was 0.09 lower than the initial value (Figure 2).

3.2. Peat Surface Elevations

[24] The peat surface elevation at all locations was influenced by the water table level, being greatest at the LL site, with a range of 10–12 cm (Figure 1). In comparison, surface level fluctuation had a range of about 6 cm at UL and 2 cm at R. Compression and expansion was observed in all peat layers, although some layers appeared more compressible than others. For example, at the 50 cm depth, the amplitude between lowest-level and highest-level sensor elevation during the measurements was about 9 cm in LL, 3.5 cm in UL, and about 1 cm in R. The volume change was also quite variable among the layers in the LL profile with the greatest changes between 50–70 cm and 20–30 cm depth. These LL layers were also the most variable compared to the automatically monitored UL and R profiles. The manual peat surface elevation measurements confirmed that there was a substantial difference between the three subsites, as well as varia-

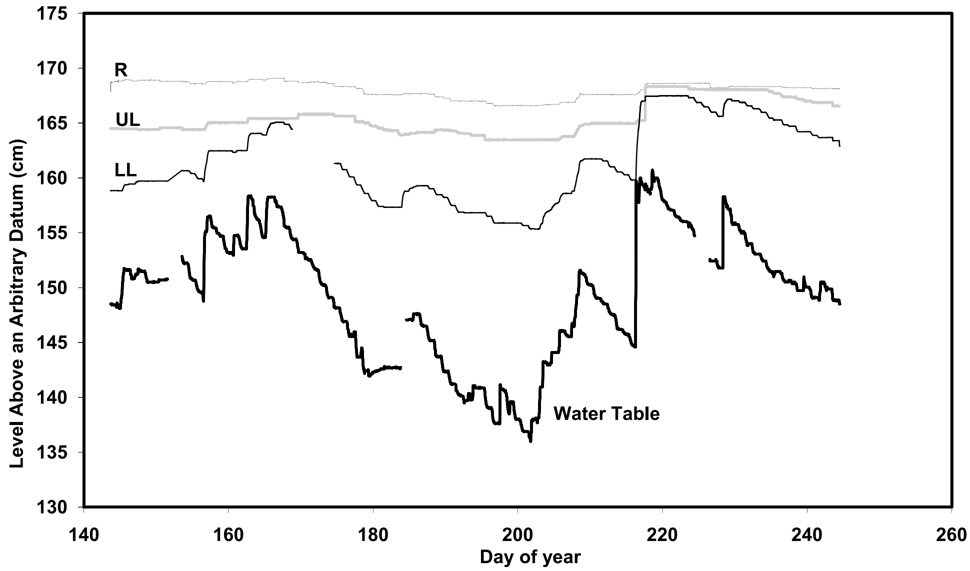

Figure 1. Water table position and low lawn (LL), upper lawn (UL), and ridge (R) surface level elevation. Levels are heights above an arbitrary datum.

tion within them (Figure 3). The biggest differences between the LL and UL group were in the layers below 40 cm depth.

[25] Volume changes in all layers generally responded on the same day as the rain event, but the delay in the response of the peat volume resulted in hysteresis (Figure 4). On a seasonal time scale, the peat surface level was lower in the beginning of the season for a given water table, compared to midseason (1.5–2 cm higher at LL surface) and after the major rain event at DOY 217 (4 cm higher at LL surface).

3.3. Peat Properties and Compressibility

[26] Depth-integrated compressibility, determined as the season-averaged slopes in the relationship between the peat surface level and the water table level, was significantly different between microforms (one-way ANOVA, F = 43.95, p <0.001) and followed the trend LL (mean ± standard deviation; 0.45 ± 0.11) > UL (0.28 ± 0.04) > R (0.09 ± 0.02) (Figure 5). Depth-integrated bulk density was also significantly different between all microforms (ANOVA, F = 76.18, p <0.001) and was greatest at R (0.068 ± 0.007 g cm^{-3}) and was 0.048 ± 0.002 and 0.036 ± 0.002 g cm^{-3} at UL and LL, respectively.

[27] Grouping all data, the general linear model shows significant differences in both compressibility and bulk density between microforms and depths (Table 1). Compressibility in the surface (10 cm) and deep layers (85 cm) were not significantly different and were significantly lower than the middle depths (30–50 cm) of the peat profile (Figure 5), while bulk density increased throughout the peat profile. Interestingly total root biomass was greatest in the 30–40 cm layer (data not shown). We also found that while there were often great variations in peat strength among the profiles, we found that peat strength (penetrometer hits cm^{-1}) generally increased with depth at all microforms and was lowest for the LL site (Figure 6).

[28] We found depth integrated compressibility was significantly correlated to peat thickness (Pearson correlation, r = −0.825, p < 0.001), distance to hollow (r = −0.907, p < 0.001), von Post decomposition (r = −0.508, p < 0.003), and peat strength (penetrometer hits) (r = − 0.662, p < 0.003). The compressibility did not correlate well to the amount of rigid roots or to the total amount of roots in the profile.

3.4. Entrapped Gas Content

[29] The volumetric gas content increased during the season with maximum gas contents at the end of the season

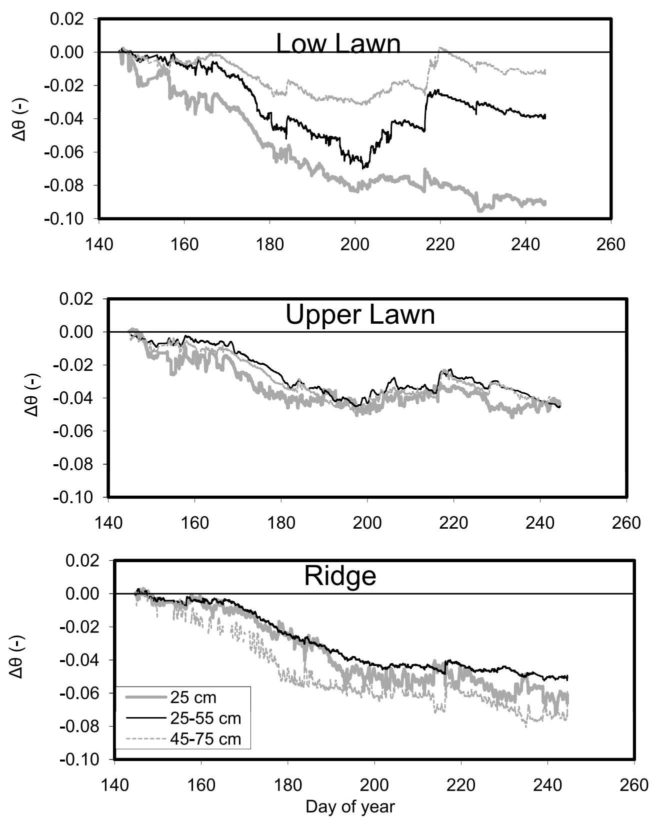

Figure 2. Change in volumetric water content at the low lawn (LL), upper lawn (UL), and ridge (R).

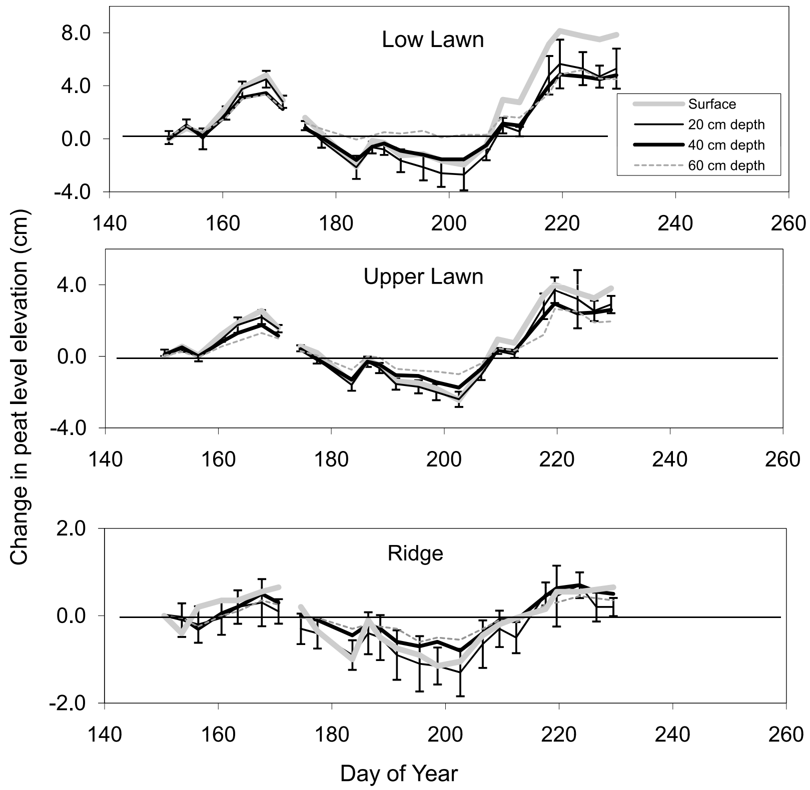

Figure 3. Change in peat level elevation from the start of measurements for the manually monitored level sensors installed at 0, 20, 40, and 60 cm depth. The plots represent the median level of six profiles in each profile (subplot) group. The error bars represent the standard deviation at 20 cm depth.

corresponding to 30 mm of water storage in R and 20 mm in LL and UL profiles. Compared to the changes in θ caused by changes in peat volume, the gas content changes seem to be a more important process (Table 2 and Figure 7). The porosity seldom varied by more than 0.01 and thus the calculated gas content in the "saturated" soil varied inversely to, but at the same magnitude as, water content variation. The calculated volumetric gas content (γ) increased from the beginning of the measurements until midsummer at all measured locations. At some locations, γ increased almost continuously all summer with only small sudden changes (Figure 7, LL25 cm, all R levels). At other sites, γ either leveled out or showed small gradual changes for the period from DOY 190 to DOY 216, during which there was a drop of about 0.01 followed by a gradual increase again until the end of the measurements.

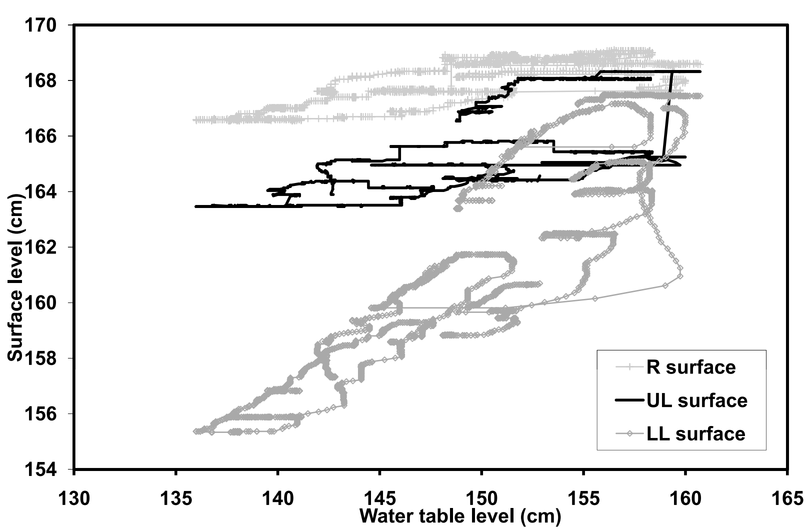

Figure 4. Variation of peat surface level with water table position variation (elevations above an arbitrary datum) for the low lawn (LL), upper lawn (UL), and ridge (R).

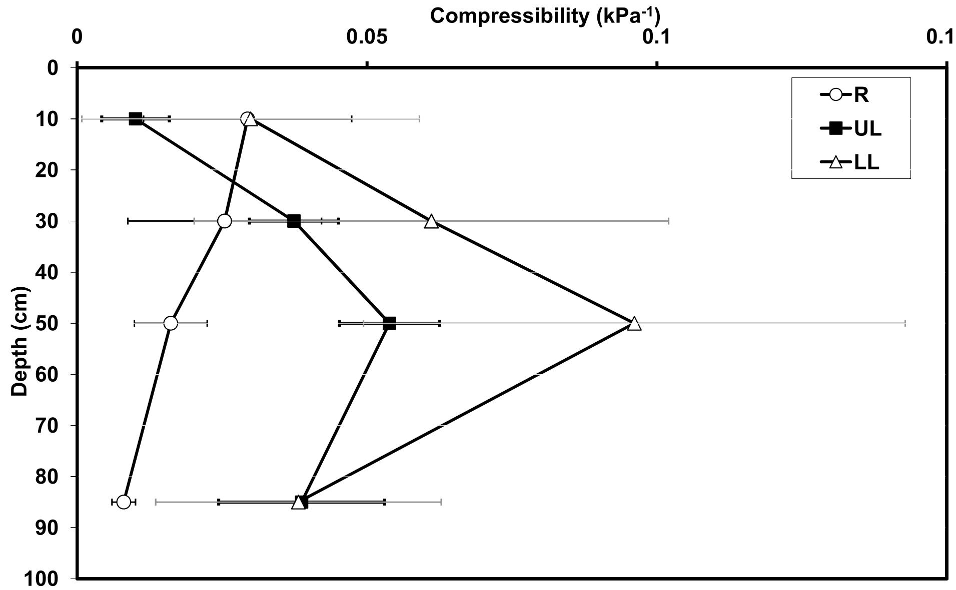

Figure 5. The average, minimum, and maximum penetrometer hits per centimeter for the low lawn (LL), upper lawn (UL), and ridge (R) sites.

3.5. Pore Water Pressure

[30] The pressure sensor at 25 cm depth in the R profile showed a response (Figure 7) very similar to the water table at LL (Figure 1). During rain events following longer dry spells the water pressure at 25 cm increased with a short peak and a subsequent drop to LL water table level. At the 40 cm depth, the pressure began to show erratic fluctuations beginning about DOY 170 that were not evident in the water table nor related to rain inputs. At 60 cm depth, the pressure began to rise at DOY 170 and continued its general rise until the end of the measurement period, also apparently unrelated to the water table response or pattern of rain.

3.6. Total Water Storage in the "Saturated" Zone

[31] We determined the change in water storage associated with dilation storage and gas formation (calculated from changes in peat volume and the changes in θ). The water storage change associated with dilation storage and gas formation was substantial for all three subsites (Figure 8a) with the greatest change in water storage observed in LL, where below 20 cm depth, it ranged from −63.5 to +67.4 mm from its initial state. When only the dilation storage in the LL profile is considered (calculated from changes in peat volume only), change in water storage ranged from −40.1 and +87.2 mm and was similar to the water budget ($P - E$), that

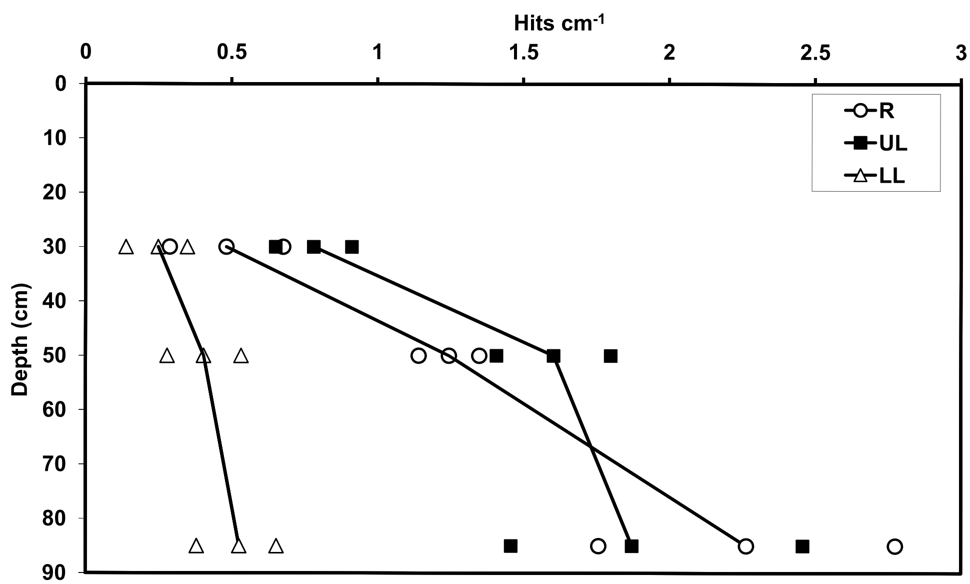

Figure 6. Variation of the calculated compressibility with depth for the low lawn (LL), upper lawn (UL), and ridge (R) sites. The symbols represent the median in each group, while the horizontal error bars represent the standard deviation within each group.

Table 1. Results of a General Linear Model[a]

Factor	Compressibility			Bulk Density		
	dF	*F*	*p*	*dF*	*F*	*p*
Microform	2	**14.72**	<0.0001	2	**73.56**	<0.0001
Depth	3	**6.56**	0.001	3	**4.71**	0.005
Microform × depth	6	2.04	0.076	6	1.35	0.252
Error	52			56		

[a]According to a repeated measures design using parameters to predict peat compressibility and bulk density. Significant higher-level predictors are marked in bold ($p < 0.05$).

ranged between −33 and +73 mm. The water storage in the UL profile was also well linked to the water budget, although the dilation storage was more positively skewed with a minimum at −5.0 mm and maximum at 56.7 mm, whereas the total water storage (gas + dilation) varied between −26.2 and +39.3 mm. The R profile dilation storage varied much less (−21.9 to +3.6 mm), whereas the total storage below 20 cm depth ranged between −46.0 and +2.0 mm. The volume change responses were often fairly quick except perhaps during rain events that occurred following longer dry spells.

4. Discussion

[32] The differences in peat movement between the subsites were clear despite the water table variation being similar over the transect. Water table amplitude at R was only 4 cm greater than at LL. The water table was generally in the near surface zone in the hollow LL area, and it can be assumed that the water table was flat in the lower end of the transect. The difference in the water table level most probably developed in the ridge, because the peat in the ridge has a lower saturated hydraulic conductivity (K_{sat}) [*Whittington and Price*, 2006]. This is because K_{sat} decreases sharply with depth and the ridge surface is higher.

[33] The difference in peat properties such as bulk density and compressibility observed among microforms was linked to variability in hydrology, including water storage and gas entrapment, along the transect. This spatial variability in hydrophysical properties likely has important implications for peatland ecology and development, and therefore, we suggest that it should be incorporated in peatland ecosystem models.

4.1. Subsidence and Water Storage

[34] Water storage changes calculated from the changes in peat volume and volumetric water content (Figure 8a) were consistently larger than those determined by volume change alone (Figure 8b). It is evident that the accumulation of biogenic gas displaces water from the matrix and should be accounted for when tracking water storage changes. The general buildup of gasses over the season may explain the hysteresis observed in the volume change data (Figure 4), where the surface elevation was higher later in the season for a given water table. Hysteresis in the relationship between surface elevation and water table has also been observed elsewhere. In a New Zealand peatland, *Fritz et al.* [2007] noted higher surface elevations in the wet period for a given water table. Moreover, *Kennedy and Price* [2005] suspected winter freezing "reset" the compressibility of peat, such that volume changes were more responsive following spring thaw than during the summer.

[35] The greatest water storage changes were registered in LL, where the peat was most compressible (Figure 5) and had the least strength (Figure 6), closely approximating the theoretical water storage change ($P - E$). In contrast, the smallest changes were in the ridge (R), where the peat is more rigid. The consequence is that the surface elevation in LL lies consistently nearer the water table than UL or R (Figure 1) [see also *Whittington and Price*, 2006]. The implications are that wetter peat is sustained at LL, which may promote evaporation losses and favor more hydrophilic plant species such as *R. alba*. Moreover, it is essential that a proper accounting of water storage change is done to close the water budget [cf. *Price and Schlotzhauer*, 1999]. The

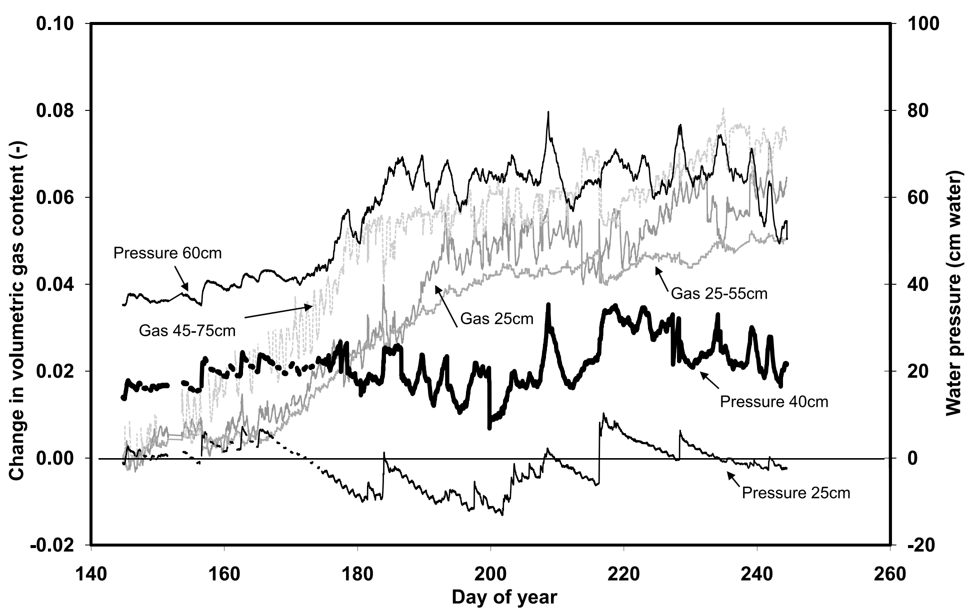

Figure 7. Change in volumetric gas content from the beginning of measurements and pore water pressure at different depths in the ridge (R) profile.

Table 2. Maximum Change in Volumetric Gas Content ($\Delta\gamma$)[a]

	Lower Lawn (LL)			Upper Lawn (UL)			Ridge (R)		
Depth (cm)	25	25–55	45–75	25	25–55	45–75	25	25–55	45–75
Max $\Delta\gamma$	0.091	0.070	0.030	0.049	0.050	0.051	0.073	0.052	0.080
Day of year	229	203	202	197	244	198	242	239	234

[a]From the start of the measurement period (DOY = 141) and the day of the year when the maximum gas content was recorded. $\Delta\gamma$, volumetric gas content.

water storage changes associated with volume change is also directly correlated to the hydraulic conductivity of peat, the most compressible soils being the most strongly affected [*Price*, 2003].

4.2. Volumetric Gas Content

[36] The rate of bubble volume increase was similar to other field studies [*Strack et al.*, 2006] and laboratory experiments [*Kellner et al.*, 2006; *Baird et al.*, 2004]. The patterns of gas volume variation were not well correlated with temperature. The bubble volume development during the season was greater than could be explained with the ideal gas law and Henry's law for the observed temperature change ($\Delta\gamma \leq 0.005$). We attribute the measured change in γ to increased gas production in the peat. However, we caution that degassing could have been caused during installation

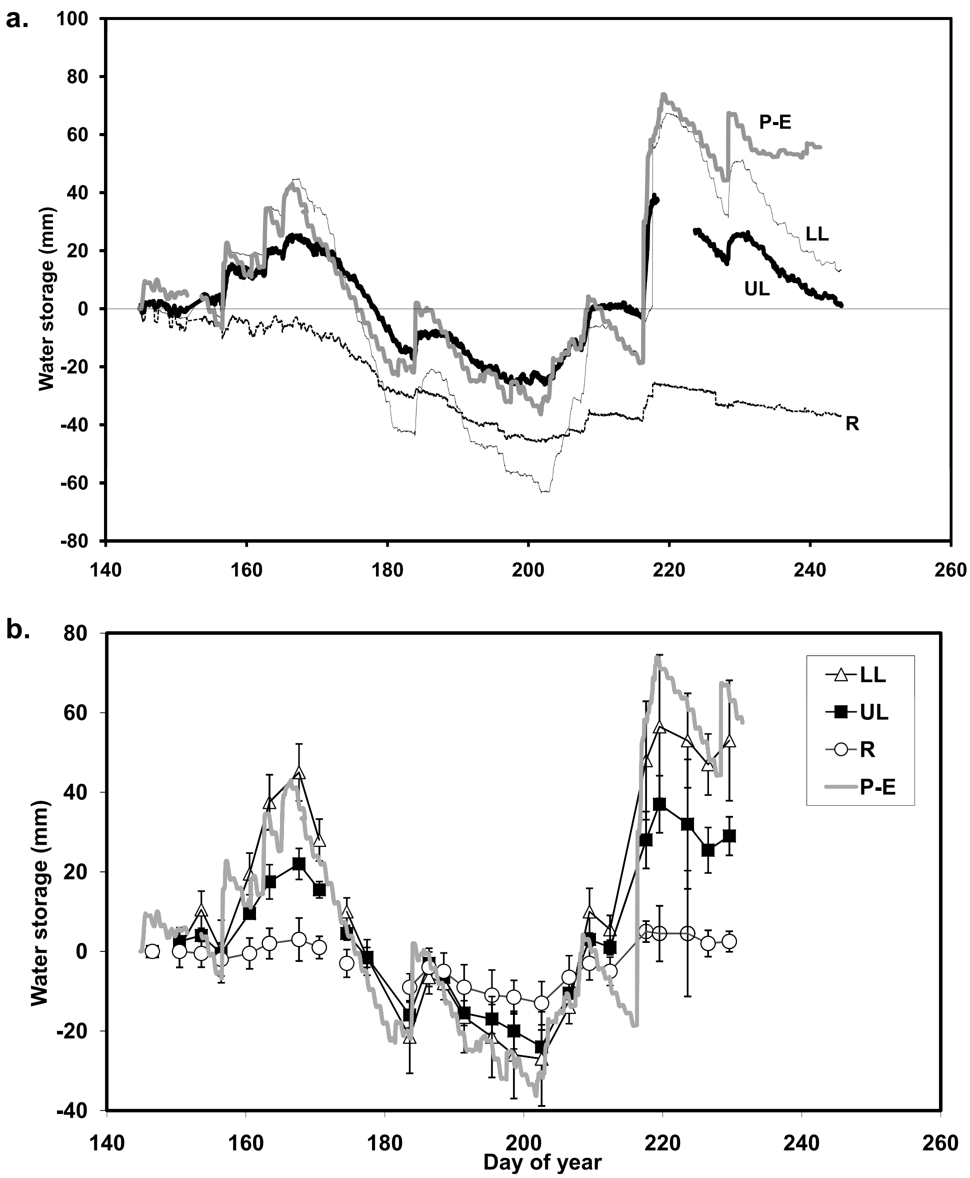

Figure 8. Calculated water storage below 20 cm depth in the low lawn (LL), upper lawn (UL), and ridge (R) profiles and the term of accumulated precipitation (P) minus evapotranspiration (E) from (a) changes in peat volume and the changes in volumetric water content and (b) by dilation.

of the probes, followed by a subsequent gas buildup to the peat gas bubble holding capacity. However, since we have expressed gas volumes as a change from the initial condition, it is unlikely that absolute gas volumes have been overestimated. There was a drop in the gas content of the LL and the UL profiles of about 0.02 following the rain event on DOY 216. This variation in gas content cannot be explained by the variation of atmospheric pressure or water table levels, which would have caused effects about 1 order of magnitude smaller than the observed, but ebullition and some redistribution of gas bubbles in the peat may have occurred during the large rainstorm at DOY 216 because of changes in pore sizes, allowing bubbles to move. This possibility is in line with the view of *Coulthard et al.* [2009] that suggests that gas movement and release within and from peat is affected by how bubbles are trapped. Nevertheless, the LL 25 cm probe did not indicate any substantial changes at DOY 216, which could be because it was only monitoring θ at 25 cm whereas the other probes in the profile monitored θ through 30 cm depth and distribution of gas throughout the peat profile is likely nonuniform.

[37] The gas content changes decreased with depth at the LL profile but not at the UL and R profiles. The gas content increased with time in a similar way among the probes. The total uncertainty of the changes is less than 0.01, and the trends (both short term and long-term changes) are considered to be real. By changing α from 0.35 to 0.2 or to 0.6 changes the absolute value of water content by 2.2% and 4.5%, respectively, but the slope change was only 0.8% and 1.1%, respectively. The changes displayed here can thus be considered accurate with a probable error of less than 1%. The low measured water content at, e.g., UL 25 cm may look peculiar, and we cannot completely explain this low value. Nevertheless, a similar value was measured with another technique in another experiment with peat taken from the same area as the UL profiles [*Kellner et al.*, 2006], which makes us believe that this measurement is not erroneous.

4.3. Gas Fluxes and Volume Dynamics

[38] Even if it is assumed that the initial increase of gas bubble volumes is an artifact, we may still say that the variations after DOY 200 are representative for the monitored profiles. Especially following the rain event on DOY 216, most γ values dropped about 0.02 units, which for the vertical probes mean $0.02 \times 0.3\ m^{-3}\ m^{-2} = 6\ L\ m^{-2}$ gas. The rate of increase before DOY 200 was about 0.001 d^{-1}, which corresponds to (if we assume the active peat to be 1 m thick) a gas production of 1 L $m^{-2}\ d^{-1}$. If we assume 50% of these bubbles consist of methane, it corresponds to a realistic minimum production rate of 5 $\mu g\ CH_4\ g^{-1}\ d^{-1}$. The probable production rate is greater since some of the produced gas escapes. While CH_4 gas emissions were not measured at this hollow ridge transect, flux measurements at a similar site less than 100 m away were <250 mL $m^{-2}\ d^{-1}$ [*Strack et al.*, 2006].

4.4. Peat Compressibility, Water Storage, and Ecosystem Function

[39] We could not find any clear correlations between the calculated m_v at individual profile layers and any other examined peat properties at the same layer. However, when average peat profile characteristics were considered, von Post humification, peat thickness (i.e., microform type), peat strength, and distance from the hollow were all correlated to compressibility. This suggests that the location in relation to the microtopographical elements, such as the hollow, or overall peat thickness may explain some of the spatial variation of the compressibility. It seems the peat morphology is self-reinforcing and supports the theory that there is a positive feedback in the microform and ecological development [*Belyea and Clymo*, 2001]. Thus, there are probably some factors not included in this study that are of great importance for the peat surface fluctuation. The height of the peat surface reflects the peat rigidity, and there is probably a connection between the surface species composition and the rigidity [*Whittington et al.*, 2007]. The *Sphagnum* moss species at the ridge is fairly tolerable to drought as its capacity to transport and hold water is better than lawn *Sphagnum* species [*Titus and Wagner*, 1984]. It seems that the more rigid structure of the ridges is maintained at depth despite different degrees of decomposition. This structure also seems more difficult to penetrate and the ridge profiles generally had a higher bulk density and higher degree of decomposition. The species in the lawns and hollow on the other hand are more competitive in wet conditions but are not durable to droughts as they dry quickly when situated more than a few centimeters over the water table. The plant communities in the lower and wetter areas thus benefit from being semifloating to floating (i.e., highly compressible).

[40] Interestingly it was not in the surface layers that LL differed from the other sites but in the 40–60 cm layer. The structure of the living plants and the poorly humified matter in the top layers therefore does not appear to be critical for the profile "squishiness." Similar to floating mat peatland ecosystems, the top 20 cm of the profile may "float" up and down with the water table fluctuation while the top layers themselves might be fairly rigid. However, it is worth noting that the surface elevation changes noted here reflect changes in pore water pressure in the peat including the effect of gas pocket compressibility, modulated by the character of the peat [*Whittington et al.*, 2007]. Surface elevation changes in true floating mat systems respond strongly to water level fluctuations but can also be influenced by methane accumulation and release [*Fechner-Levy and Hemond*, 1996].

4.5. Implications for Peatland Development

[41] Others have also observed that hummock peat is more dense and less permeable than lawn and hollow peat [*Lapen et al.*, 2005]. Thus, the hummocks and ridges can be regarded as barriers against lateral water flow, keeping the water table high within the peatland [*Quinton and Roulet*, 1998; *Swanson and Grigal*, 1988]. The water table had a slope from the hollow toward the ridge with a smaller gradient during wet periods. In this study, we found differences in compressibility and gas contents that further indicate a reduction of water flow through hummocks and ridges.

[42] Peatland microforms are believed to be secondary features on peatlands [*Foster et al.*, 1988; *Belyea and Lancaster*, 2002] with their distribution and development likely the result of autogenic processes linked to the overall development of the peatland [*Foster et al.*, 1988; *Eppinga et al.*, 2008]. Indeed contemporary differences in carbon accumulation among peatland microforms [e.g., *Waddington and*

Roulet, 2000] are viewed to alter overall peatland development. Moreover, *Belyea and Baird* [2006] suggest that microforms and their associated hydraulic properties (e.g., hydraulic conductivity) may affect peatland development over very long time scales through internal feedbacks termed "ecological memory." The self-organization of hummocks of low hydraulic conductivity into ridges can have even larger peatland development impacts [*Lapen et al.*, 2005; *Belyea and Baird*, 2006]. It is believed that the microforms grow and contract in response to changes in external forcings (e.g., climate) [*Belyea and Clymo*, 2001]. Our results demonstrate that lawn (LL and UL) compressibility is significantly greater than the adjacent ridges, suggesting that their hydraulic properties (water storage and hydraulic conductivity) change more within a growing season in response to changes in $P - E$ and that the ecosystem water losses (runoff and evapotranspiration) and potentially species distribution are also most likely to change in response to multiyear drought. *Whittington and Price* [2006] noticed a 3–5 order of magnitude decrease in lawn saturated hydraulic conductivity with subsidence following water table drawdown in a Québec poor fen. This suggests under drought that large areas of lawns may also serve the same function as ridges or "curtains" of low K_{sat} hummocks [e.g., *Belyea and Baird*, 2006] by altering water movement, evapotranspiration, and peatland development through differences in their peat properties. Recent ecohydrological modeling research suggests that peatland development is controlled by differences in microform evapotranspiration rates [*Eppinga et al.*, 2008], which in turn result in differences in nutrient availability. We argue that the differences in microform peat deformation and other hydrophysical properties observed in this study must be incorporated in this and other ecohydrological models to correctly model the effects of land use and climate change on peatland hydrology and peatland development.

5. Conclusions

[43] We examined the spatial and temporal variation in peat surface movement, compressibility, strength, and gas content along a LL, UL, and R transect. We found that peat profile compressibility was significantly higher at LL compared to UL and R and could be related to von Post, bulk density, distance to hollow, and peat thickness. This suggests that both microform type/local conditions and the spatial arrangement of these microforms are important for controlling hydrophysical properties at a given location. Differences in compressibility had an effect on water storage with the largest changes observed at LL followed by UL and R. This has implications on surface moisture conditions with potential ecological consequences. Including estimates of entrapped gas buildup had a significant impact on storage estimates. Our findings suggest that there are likely strong hysteretic responses between surface-level and water table position on peat hydraulic conductivity and evaporation and indirectly on whole peatland ecosystem function. Given these important cross-scale feedbacks and that this exploratory study research design was pseudoreplicated, we suggest that these relationships and the magnitude of these intermicroform differences be investigated in a variety of peatlands that differ in vegetation type, microform development and organization, and regional climate.

[44] **Acknowledgments.** Funding for this research was provided by a Premier's Research Excellence Award from the Ontario Ministry of Research and Innovation to J.M.W. and NSERC Discovery grants awarded to J.M.W. and J.S.P. We thank Nirom Peat Moss, Inc., for allowing access to the research site. We wish to thank Pete Whittington and Monique Waller for assistance in the field and Giles Turnbull for assistance in the laboratory.

References

Baird, A. J., C. W. Beckwith, S. Waldron, and J. M. Waddington (2004), Ebullition of methane-containing gas bubbles from near-surface *Sphagnum* peat, *Geophys. Res. Lett.*, *31*, L21505, doi:10.1029/2004GL021157.

Belyea, L., and A. Baird (2006), Beyond "the limits to peat bog growth": Cross-scale feedback in peatland development, *Ecol. Monogr.*, *76*, 299–322.

Belyea, L. R., and J. Lancaster (2002), Inferring landscape dynamics of bog pools from scaling relationships and spatial patterns, *J. Ecol.*, *90*(2), 223–234.

Belyea, L. R., and R. S. Clymo (2001), Feedback control of the rate of peat formation, *Proc. R. Soc. Long Series B*, *268*, 1315–1321.

Bilskie, J. (1997), Using dielectric properties to measure soil water content, *Sensors Mag.*, *14*, 26–32.

Birchak, J. R., C. G. Gardner, J. E. Hipp, and J. M. Victor (1974), High dielectric constant microwave probes for sensing soil moisture, *Proc. IEEE*, *62*, 93–98.

Coulthard, T., A. J. Baird, J. Ramirez, and J. M. Waddington (2009), Modeling methane dynamics in peat: importance of shallow peats and a novel reduced-complexity approach for modelling ebullition, in *Carbon Cycling in Northern Peatlands*, edited by A. J. Baird et al., Geophysical Monograph Series, American Geophysical Union, Washington, D. C.

Eppinga, M., M. Rietkerk, W. Borren, E. D. Lapshina, W. Bleuten, and M. J. Wassen (2008), Regular surface patterning of peatlands: Confronting theory with field data, *Ecosystems*, *11*, 520–536.

Fechner-Levy, E. J., and H. Hemond (1996), Trapped methane volume and potential effects on methane ebullition in a northern peatland, *Limnol. Oceanogr.*, *41*, 1375–1383.

Foster, D. R., G. A. King, P. H. Glaser, and H. E. Wright Jr. (1983), Origin of string patterns in boreal peatlands, *Nature*, *306*, 256–258.

Foster, D. R., H. E. Wright Jr., M. Thelaus, and G. A. King (1988), Bog development and landform dynamics in central Sweden and south-eastern Labrador, Canada, *J. Ecol.*, *76*, 1164–1185.

Fritz, C., D. Campbell, and L. A. Schipper (2007), Oscillating peat surface levels in a restiad peatland, New Zealand – magnitude and spatiotemporal variability, *Hydrol. Processes*, *22*, 3264–3274, doi:10.1002/hyp.6912.

Gorham, E. (1991), Northern peatlands: Role in the carbon cycle and probable response to climatic warming, *Ecol. Appl.*, *1*, 182–195.

Gorham, E. (1995), The biogeochemistry of northern peatlands and its possible responses to global warming, in *Biotic Feedbacks in the Global Climatic System: Will the Warming Feed the Warming?*, edited by G. M. Woodwell and F. T. MacKenzie, pp. 169–187, Oxford Univ. Press, New York.

Kellner, E., and L. C. Lundin (2001), Calibration of time domain reflectometry for water content in peat soil, *Nordic Hydrol.*, *32*, 315–332.

Kellner, E., J. M. Waddington, and J. S. Price (2005), Dynamics of biogenic gas bubbles in peat: Potential effects on water storage and peat deformation, *Water Resour. Res.*, *41*, W08417, doi:10.1029/2004WR003732.

Kellner, E., A. J. Baird, M. Oosterwoud, K. Harrison, and J. M. Waddington (2006), Effect of temperature and atmospheric pressure on methane (CH_4) ebullition from near-surface peats, *Geophys. Res. Lett.*, *33*, L18405, doi:10.1029/2006GL027509.

Koerselman, W. (1989), Groundwater and surface water hydrology of a small groundwater-fed fen, *Wetlands Ecol. Manage.*, *1*, 31–43.

Price, J. S. (2003), The role and character of seasonal peat soil deformation on the hydrology of undisturbed and cutover peatlands, *Water Resour. Res.*, *39*(9), 1241, doi:10.1029/2002WR001302.

Price, J. S., and D. A. Maloney (1994), Hydrology of a patterned bog-fen complex in southeastern Labrador, Canada, *Nordic Hydrol.*, *25*(5), 313–330.

Price, J. S., and S. M. Schlotzhauer (1999), Importance of shrinkage and compression in determining water storage changes in peat: the case of a mined peatland, *Hydrol. Processes*, *13*, 2591–2601.

Price, J. S., J. Cagampan, and E. Kellner (2005), Assessment of peat compressibility: is there an easy way? *Hydro. Processes*, *19*, 3469–3475.

Pyatt, D. G., and A. J. John (1989), Modelling volume changes in peat under conifer plantations, *Eur. J. Soil Sci.*, *40*, 695–706.

Quinton, W. L., and N. T. Roulet (1998), Spring and summer runoff hydrology of a subarctic patterned wetland, *Arc. Alp. Res.*, *30*, 285–294.

Rydin, H., and J. K. Jeglum (2006), *The Biology of Peatlands*, 352 pp., Oxford Univ. Press, Oxford.

Strack, M., and T. Mierau (2010), Evaluating spatial variability of free-phase gas in peat using ground-penetrating radar and direct measurement, *J. Geophys. Res.*, *115*, G02010, doi:10.1029/2009JG001045.

Strack, M., E. Kellner, and J. M. Waddington (2005), Dynamics of biogenic gas bubbles in peat and their effects on peatland biogeochemistry, *Global Biogeochem. Cycles*, *19*, GB1003, doi:10.1029/2004GB002330.

Strack, M., E. Kellner, and J. M. Waddington (2006), Effect of entrapped gas on peatland surface level fluctuations, *Hydrol. Processes*, *20*, 3611–3622.

Swanson, D. K., and D. F. Grigal (1988), A simulation model of mire patterning, *Oikos*, *53*, 309–314.

Titus, J. E., and D. J. Wagner (1984), Carbon balance for two *Sphagnum* mosses: Water balance resolves a physiological paradox, *Ecol.*, *65*, 1765–1774.

Turunen, J., E. Tomppo, K. Tolonen, and A. Reinikainen (2002), Estimating carbon accumulation rates of undrained mires in Finland – application to boreal and subarctic regions, *The Holocene*, *12*, 69–80.

Waddington, J. M., and N. T. Roulet (2000), Carbon balance of a boreal patterned peatland, *Global Change Biol.*, *6*, 87–97.

Whittington, P. N., and J. S. Price (2006), The effects of water table drawdown (as a surrogate for climate change) on the hydrology of a fen peatland, Canada, *Hydrol. Processes*, *20*, 3589–3600.

Whittington, P., M. Strack, R. van Haarlem, S. Kaufman, P. Stoesser, J. Maltez, J. S. Price and M. Stone (2007), The influence of peat volume change and vegetation on the hydrology of a kettle-hole wetland in Southern Ontario, Canada, *Mires and Peat*, *2*, 9.

E. Kellner and J. M. Waddington, School of Geography and Earth Sciences, McMaster University, 1280 Main St. West, Hamilton, ON L8S 4K1, Canada. (jmw@mcmaster.ca)

J. S. Price, Department of Geography and Environmental Management, University of Waterloo, 200 University Ave. West, Waterloo, ON N2L 3G1, Canada.

M. Strack, Department of Geography, University of Calgary, 2500 University Dr. Calgary, AB T2N 1N4, Canada.